DOE/ET/53088-66 IFSR #66

CURVATURE-DRIVEN INSTABILITIES IN THE ELMO BUMPY TORUS (EBT)

H. Abe, H. Berk, C. Cheng, M. Rosenbluth, J. W. Van Dam
Institute for Fusion Studies

D. A. Spong, N. A. Uckan
Oak Ridge National Laboratory

T. M. Antonsen, Jr., Y. C. Lee
Department of Physics and Astronomy
University of Maryland

K. T. Tsang, P. J. Catto, X. S. Lee
Science Applications, Inc.

K. T. Nguyen, T. Kammash
Dept. of Nuclear Engineering, University of Michigan

CURVATURE-DRIVEN INSTABILITIES IN THE ELMO BUMPY TORUS (EBT)

H. Abe*, H. L. Berk, C. Z. Cheng**, M. N. Rosenbluth, J. W. Van Dam
Institute for Fusion Studies
The University of Texas at Austin
Austin, Texas 78712 USA

D. A. Spong, N. A. Uckan
Oak Ridge National Laboratory
Oak Ridge, Tennessee 37830 USA

T. M. Antonsen, Jr., Y. C. Lee
Department of Physics and Astronomy
The University of Maryland
College Park, Maryland 20742 USA

K. T. Tsang, P. J. Catto, X. S. Lee
Science Applications, Inc.
Plasma Research Institute
Boudler, Colorado 80302 USA

K. T. Nguyen, T. Kammash
Department of Nuclear Engineering
The University of Michigan
Ann Arbor, Michigan 48109 USA

Permanent Addresses for:

* H. Abe: Department of Electronics, Kyoto University, Kyoto, Japan.

** C. Z. Cheng: Plasma Physics Laboratory, Princeton University, Princeton, New Jersey, 08544 USA

Presented at
International Atomic Energy Agency
9th International Conference on Plasma Physics and
Controlled Nuclear Fusion
September 1-8, 1982
Baltimore, Maryland, USA
IAEA-CN-41/T-6-1

Abstract

Curvature-driven instabilities are analyzed for an EBT configuration which consists of plasma interacting with a hot electron ring whose drift frequencies are larger than the growth rates predicted from conventional magnetohydrodynamic (MHD) theory. Stability criteria are obtained for five possible modes: the conventional hot electron interchange, a high-frequency hot electron interchange (at frequencies greater than the ion-cyclotron frequency), a compressional instability, a background plasma interchange, and an interacting pressure-driven interchange. A wide parameter regime for stable operation is found, which, however, severely deteriorates for a band of intermediate mode numbers. Finite Larmor radius effects can eliminate this deterioration; moreover, all short-wavelength curvature-driven modes are stabilized if the hot electron Larmor radius ρ_h satisfies $(k_\perp \rho_h)^2 > 2\Delta/[R\beta_h(1 + P_\parallel'/P_\perp')]$, where $k_\perp$ is the transverse wavenumber, Δ is the ring half-width, R is the mid-plane radius of curvature, β_h is the hot electron beta value, and P' is the pressure gradient. Resonant wave-particle instabilities predicted by a new low frequency variational principle show that a variety of remnant instabilities may still persist.

I. INTRODUCTION

Recently, there have been extensive investigations[1-6] of the special stability physics associated with the Elmo Bumpy Torus (EBT) configuration in which the dynamics of the hot electrons can decouple from the background plasma and form a diamagnetic well that produces stable confinement. For the success of this method, it is vital that the system behave far differently than is predicted from the conventional MHD description, where the bumpy torus configuration appears to be highly unstable. Indeed, it is found that the system responds far differently from an MHD theory if both of the following conditions are fulfilled:

(1) The curvature-drift frequency of the hot component is roughly greater than the growth rate predicted from a conventional MHD calculation;

(2) The core beta, β_c, is sufficiently small, viz. $\beta_c \lesssim 2(\Delta/R)(1 + P'_{\parallel h}/P'_{\perp h})$ where Δ is the one-half thickness at the hot annulus, R the radius of curvature at the annulus, and P'_h the hot electron pressure gradient.

When these two conditions are fulfilled, one still finds the possibility of instability which can be predicted from either variational or modal calculations. Although remnant instabilities can always be found, with probably low saturation levels, there exist broad parameter ranges where gross instability can be found. Troublesome instability islands arise when positive and negative energy modes match to give new types of instabilities. Further, the stability picture is altered profoundly by the consideration of finite Larmor radius of the background ions and the hot electrons where it is found that moderate electron finite Lamor radius (FLR) effects can broaden instability regimes, while stronger FLR effects are stabilizing.

In this work we will summarize the various approaches that have been used to study the stability of curvature-driven modes in EBT, and we will discuss some of their implications for present and future machines.

II. VARIATIONAL ANALYSIS

A new variational principle was developed to study the stability of low-frequency (less than the magnetic drift frequency) perturbations of a hot electron ring-plasma system in the guiding center limit. This principle was derived from the drift kinetic equation including the electrostatic potential[1] and also, at marginal stability, from the magnetic moment, action, and flux adiabatic invariants.[2] If the guiding center distribution functions decrease monotonically with energy ($\partial F/\partial E < 0$, positive dissipation), it can be shown by the Nyquist technique that $\Delta W_0 < 0$ is a necessary and sufficient condition for instability,[3] where ΔW_0 is the perturbation potential energy at zero frequency:

$$\Delta W_0 = \frac{1}{2}\int d^3r \left[\sigma|\vec{Q}_\perp|^2 + \tau_*|\hat{Q}_\parallel|^2 + \sigma\ J_\parallel \vec{b}\cdot(\vec{\xi}*\times\vec{Q}_\perp)\right]$$

$$- (\vec{\xi}*\cdot\vec{\kappa})\left(\vec{\xi}\cdot\hat{\nabla}P_\parallel + \frac{B^2\sigma^2}{\tau_*}\vec{\xi}\cdot\vec{\kappa} - B\sigma\ \vec{\xi}\cdot\nabla B\right)$$

$$+ \sum_j \int d\Gamma f_L \left[Mv_\parallel^2\vec{\xi}*\cdot\vec{\kappa} + \left(\mu - q\frac{\partial\rho/\partial B}{\partial\rho/\partial\phi}\right)\left(\hat{Q}_\parallel^* + \frac{\sigma}{\tau_*}\vec{\xi}*\cdot\vec{\kappa}\right)\right] . \quad (1)$$

Here, $\vec{\xi}$ is the field line displacement, $\vec{Q} = \nabla\times(\vec{\xi}\times\vec{B})$ is the perturbed magnetic field, $\hat{Q}_\parallel = \vec{Q}\cdot\vec{b} + \vec{\xi}\cdot(\nabla B - \sigma B\vec{\kappa}/\tau_*)$ with $\vec{b} = \vec{B}/B$, $\tau_* = 1 + \partial P_\perp/B\partial B - (\partial\rho/\partial B)^2(\partial\rho/\partial\phi)^{-1}$ with ρ the charge density and ϕ the electrostatic potential, $J_\parallel$ is the parallel current, $\vec{\kappa} = \vec{b}\cdot\nabla\vec{b}$ is the curvature, $\hat{\nabla} = \vec{\nabla}|_{B,\phi}$, the summation Σ_j is over all species, and f_L is the Lagrangian perturbed distribution function obtained by solving the drift kinetic equation.

This principle predicts that a plasma configuration with a ring of hot electrons trapped in an unfavorable curvature region is always unstable. In particular, the plasma is interchange unstable when its pressure P_c (assumed isotropic) exceeds the limit given in the high mode number axisymmetric limit by

$$\left|\oint\frac{ds}{B}\frac{dP_{\perp h}}{d\psi}\frac{d}{d\psi}\left(\frac{P_c}{B^2}\right)\right| < \oint\frac{ds}{B}\left(\frac{\kappa}{rB}\right)\frac{d}{d\psi}\left(P_{\perp h} + P_{\parallel h}\right) \quad (2)$$

where $d/d\psi = |\nabla\psi|^{-2}\vec{\nabla}\psi\cdot\vec{\nabla}$, ψ the magnetic flux, $P_{\perp,\parallel h}$ are the hot electron pressure components, and s is the distance along a field line. This condition is the quantitative statement of violating condition (2) in the introduction.

Below the β_c limit given by Eq. (2) the nature of the instabilities alter, but ΔW_0 will still be less than zero. In this case the system is susceptible to a magnetic compressional mode, which can have extremely high growth rates if there is too much core plasma present. However, with moderate core plasma density the instability is of a resonant nature in which the positive dissipation permits negative energy modes to grow. To examine this situation, a study has been undertaken of low-mode-number instabilities in a bumpy cylinder system where the hot electron annulus is assumed to be confined to a layer of half width Δ that is much smaller than the cylinder radius a .

The displacement is written $\vec{\xi} = [(\nabla\theta\times\vec{B}/B^2)X - (\nabla\psi\times\vec{B}/B^2)Y]\exp[i(m\theta - \omega t)]$, with θ the azimuthal angle and ω the frequency. Taking variations of the finite-frequency quadratic form, which is expanded in powers of Δ/a keeping $\beta_c \sim \Delta/a$ for the core plasma pressure and $\beta_h \sim 1$ for the hot electrons, yields equations for the components X and Y. In lowest order, $X^{(0)} = 0$ while $Y^{(0)} = \partial U(\psi)/\partial\psi$ is flute-like, with $X^{(1)}(\psi,s)$ being determined from $Y^{(0)}$ and another flux function. Next order leads to an equation for $Y^{(0)}(\psi)$, which, for $\Delta/a < \beta_h < 1$, reduces to

$$\omega^2 \frac{\partial}{\partial\psi}\left[I(\psi)\,\frac{\partial U}{\partial\psi}\right] - \left(\frac{GD}{G - D}\right)U(\psi) = 0 . \qquad (3)$$

Here, $I = \oint dsB^{-1}(\rho_m r^2/m^2)$ is the inertia with ρ_m the mass density; $D = \oint dsB^{-1}(\vec{e}\cdot\vec{\kappa})[\vec{e}\cdot\nabla P_{\parallel h} + (\sigma/\tau_*)\vec{e}\cdot\nabla P_{\perp h}]$ is the hot electron interchange drive; and

$$\begin{aligned} G(\psi) = &-\oint\frac{ds}{B}\int_{ring} d\Gamma\left(\frac{\partial F_h}{\partial E}\right)_J\left(\frac{\omega}{\omega - m\omega_d}\right)\langle\mu\vec{e}\cdot\nabla B\rangle^2 \\ &+\oint\frac{ds}{B}\int_{core} d\Gamma\Bigg[(\vec{e}\cdot\nabla F_c)\langle\vec{e}\cdot\nabla(\mu B + q\phi)\rangle \\ &-\left(\frac{\partial F_c}{\partial E}\right)_\psi \sum_{n=-\infty}^{\infty}\left(\frac{\omega}{\omega - n\omega_b}\right)\left|\langle\exp(in\zeta)\vec{e}\cdot\nabla(\mu B + q\phi)\rangle\right|^2\Bigg] \end{aligned} \qquad (4)$$

where $\vec{e} = \nabla\psi/|\nabla\psi|^2$ contains finite frequency and drift resonance terms for the hot ring electrons, as well as finite core beta and bounce resonances for the background plasma. Also, $d\Gamma = 2\pi\, dE d\mu B/M^2 |v_\parallel|$ with $v_\parallel = \pm[2(E - \mu B - q\phi)/M]^{1/2}$; $2\pi/\omega_d = \oint d\theta\langle\vec{v}_d\cdot\nabla\theta\rangle^{-1}$ is the period for a drift orbit, with $\vec{v}_d = (c/qB)\vec{b}\times[Mv_\parallel^2\vec{\kappa} + \mu\nabla B + q\nabla\phi]$; $2\pi/\omega_b = \oint ds v_\parallel^{-1}$ is the bounce period; $\zeta = \omega_b\int^s ds' v_\parallel^{-1}$ is an angle-like variable; and $\langle\ldots\rangle = \oint(d\zeta/2\pi)(\ldots)$ denotes bounce averaging. The solutions of Eq. (3) describe the interchange instability and possibly a resonant version of the compressional Alfvén instability. Within this ordering scheme, the nonresonant Alfvén mode is not present. Equation (3) can be easily modified to include parallel electric field and finite ion gyro-frequency effects. The structure of Eq. (3) closely resembles the structure that arises in the radial analysis of a z-pinch model which will now be discussed.

III. RADIAL EIGENMODE ANALYSIS

The z-pinch model, with its natural curvature, is especially convenient for studying the radial mode structure. This model was self-consistently developed for eigenmodes with frequencies comparable to the ion cyclotron frequency ω_{ci} in the zero gyro-radius, flute limit.[4] Ions were treated as cold, core plasma electrons as warm, and ring electrons relativistically. The differential equation for the model is

$$\frac{d}{dr}\left\{\left[\frac{\lambda\rho_m r(1+G_1)}{1+G_1-\lambda\rho_m/k^2r^2}\right]\exp\left(2\int^r dr' H\right)\frac{d\Psi}{dr}\right\}$$

$$-\exp\left(2\int^r dr' H\right)\left[k^2\rho_m r\omega^2+\frac{(1-G_2)^2k^2B^2}{r(1+G_1)}-k^2\frac{d}{dr}\left(P_\parallel+P_\perp\right)\right.$$

$$\left.-\frac{k^2B^2}{r}\left(\sigma+G_3\right)\right]\Psi(r) = 0 \ . \qquad (5)$$

The dependent variable Ψ in Eq. (5) is related to the radial displacement $\xi_r = \Psi(r)\exp(\int^r dr' H)$, with $H = (1-G_2)/r(1+G_1) + k\omega/\omega_{ci}$. Here,

$$\begin{Bmatrix} G_1 - \dfrac{1}{B}\dfrac{\partial P_\perp}{\partial B} \\[2ex] G_2 - \dfrac{1}{B}\dfrac{\partial P_\parallel}{\partial B} \\[2ex] G_3 \end{Bmatrix} \equiv -\sum_j \frac{1}{M}\int \frac{dE\,d\mu\,B}{\gamma|p_\parallel|}\,\frac{\left(\dfrac{k}{qB}\dfrac{\partial F}{\partial r}+\omega\dfrac{\partial F}{\partial E}\right)}{\left(\omega-\dfrac{\mu k}{qMB}\dfrac{dB}{dr}+\dfrac{p_\parallel^2 k}{q\gamma MBr}\right)}\begin{Bmatrix} u^2 \\[2ex] \mu p_\parallel^2/B^2 \\[2ex] (p_\parallel^2/B)^2 \end{Bmatrix} \qquad (6)$$

with E the relativistic energy and $c^2p_\parallel^2 = E^2 - 2\mu Bc^2 - M^2c^4$. Also, $\sigma = 1 + (P_\perp - P_\parallel)/B^2$ and $\lambda = \omega^2\omega_{ci}^2/(\omega_{ci}^2-\omega^2)$.

Five types of short-wavelength modes (i.e., with radial wavenumber $k_r > \Delta^{-1}$) were found: a low-pressure core interchange mode for which the hot electrons behave as rigid and non-interacting; low-frequency ($\omega \ll \omega_{ci}$) and high-frequency ($\omega \gtrsim \omega_{ci}$) versions of hot electron interchange; a magnetic compressional Alfvén mode; and an interacting ring-plasma interchange mode. Analytical expressions for their respective stability criteria, maximum growth rates, and marginal frequencies are listed in Table I. The notation is $k_\perp^2 = k_r^2 + k^2$, $q_0 = (\gamma^2 - 1)/2\gamma\Delta R\omega_{ci}|\omega_{ce}|$ with R the radius of curvature and $T_h = (\gamma - 1)M_e c^2$ the hot electron kinetic energy, and n_h and n_i the hot electron and ion densities.

This table indicates that the description of the instability regimes roughly separates into two cases, $q_0 > 1$ and $q_0 < 1$. The case $q_0 > 1$ applies to the current EBT-S experiment where $q_0 \approx 8$ and even EBT-P where $q_0 = 2$. For reactor-like parameters $q_0 \ll 1$, $(\sim 5\times 10^{-2})$. For $q_0 \gg 1$, the stability condition for the low frequency hot electron interchange mode is automatically satisfied, but a high frequency hot electron interchange mode exists. As indicated in the table, both these modes need a sufficiently high core plasma density for stability. If $q \equiv k^2 q_0(1 - \beta_c)/k_\perp^2 < 1$, the compressional mode characteristics are independent of ω/ω_{ci}, and a sufficiently low background plasma density is needed for stability. Table I indicates that there is a substantial window for stable plasma operation except near $q = 1$, (which only arises for $q_0 > 1$) where the stability criteria for the two modes completely shrinks away the window of stability.

In the next section, we show that the stable window re-emerges when FLR effects are considered. The unstable band can be interpreted as arising from the coalescence of two stable waves: the negative energy precessional mode $\omega \equiv \omega_{cv} \equiv kq_0\omega_{ci}\Delta(1 - \beta_c)$ and drift waves obtained from the balance of the high frequency ion inertia term and the background electron $\vec{E}\times\vec{B}$ drift, which gives $\omega = (k_\perp^2/k)\Delta\omega_{ci}$. For $q_0 < 1$, it is possible to show an additional unstable band arises[7] from coalescence of the negative energy precessional mode with a shear Alfvén wave ($\omega_{cv} = k_\parallel V_A$, $V_A = B/(n_i m_i)^{1/2}$ and $k_\parallel$ is quantized in the toroidal direction).

The core plasma density is limited from above by either the compressional Alfvén wave or the interacting ring-plasma interchange mode. For low core plasma temperatures, the compressional Alfvén wave limits the background plasma density, while for higher core plasma temperatures the interacting ring-plasma interchange mode determines the upper density limit. In Fig. 1 we show numerical plots for the stability boundaries for EBT-P parameters when the core plasma is heated to the maximum design value. The parameters are B = 10 kg., $\Delta = 1.5$ cm, R = 26 cm, a = 18 cm, and $T_h = 1$ MeV, $\beta_c = 2n_cT_c/B^2$ with $T_c = 10$ keV with $k = m/r_p$, the stability plots are shown for m = 1,15,20,35,60. In these plots, the lower stability boundary comes from either the physical constraint $n_c \gtrsim n_h$ or from one of the hot electron interchange modes. The upper boundary is due to the interacting ring-plasma interchange mode. The compressional Alfvén wave instability does not arise because β_c is finite. However, considerable deterioration at high m of the stability band arises where $q \to 1$. In these plots we have chosen $k_r\Delta = 2$, a result found for the largest wavelength WKB-like modes in one simplified analytic model.

There is also a long-wavelength $(k_r\Delta \ll 1)$ version of the interacting core interchange mode. Its stability is again limited by $\beta_c \lesssim 2\Delta/R$ (we assume $P_{\parallel h} < P_{\perp h}$) , although for some parameters the core beta limit can be even less:

$$\beta_c < \frac{2\Delta}{R} \,\mathrm{Min}\left\{1, \frac{4mq_0n_c}{27a\left[1 - 2\Delta/(R\beta_h)\right]n_h}\right\} . \tag{7}$$

The latter limit may make the core beta limit somewhat more restrictive than the simple scaling.

The modes most pertinent to the reactor regime in Table I are MHD hot electron interchange, background pressure interchange (with curvature averaged over full sector), and interacting pressure mode. Boundaries for the stable operating window as a function of n_c/n_h and q_0 are shown in Fig. 2. Within the constraints that reactor parameters lie within the possible operating window for the stability and the core pressure profile inside the ring satisfies core interchange criteria, a favorable reactor design has been formulated[8] in regards to both recirculated power fraction (~ 5-10%) and total fusion power produced (~ 1000MWe).

Numerical solution of the radial differential equation [Eq. (5)] with realistic pressure and magnetic field profiles generally tends to confirm the short-wavelength local results. The eigenfunctions for the two high frequency modes peak on the outer half of the ring where $\partial P_{\perp h}/\partial\psi < 0$. For EBT-S parameters, the hot electron interchange growth rate is zero for core densities greater than $5\times10^{11} - 2\times10^{12}$ cm^{-3} , although modes with low mode numbers $(m \leqq 4)$ appear to be unstable independent of density. We have not yet been able to interpret this instability band. It may be due to the self-consistent k_r being appreciably less than $2/\Delta$ found in a simply analytical model, or due to a new mode not immediately apparent from a local WKB analysis. The compressional instability occurs at densities of at least 5×10^{13} cm^{-3}, which are well above current experimental values.

Additional relativistic effects were also examined on the basis of a slab model dispersion relation for the low frequency modes, with an anisotropic relativistic Maxwellian distribution for the hot electrons.[5] In one particular example for a shallow diamagnetic well $(\beta_h R/4\Delta = 1.5)$, when the ring is quite relativistic ($\gamma \simeq 10$) the maximum allowed core beta value for interchange stability was found to increase by 50 per cent from nonrelativistic theory. For deep wells, the relativistic effects are less significant. Also, they seem to have little effect on the low frequency hot electron interchange and compressional modes for any β_h value.

IV. FINITE LARMOR RADIUS EFFECTS

The effects of finite ion and hot electron Larmor radii on the stability of curvature-driven modes in general geometry was studied with eigenmode equations derived in the eikonal limit from a gyro-kinetic equation valid for arbitrary frequency. A set of three coupled equations--the perpendicular and parallel Ampere's law and a quasi-neutrality condition--was derived, containing Larmor radius, drift resonance, trapped particle, Landau damping, and high frequency effects. Detailed analysis has been made with the assumption that the parallel electric field is zero. For simplicity, only results in the local approximation are given here. The core interchange mode obeys the dispersion relation

$$\omega(\omega - \omega_{*i}) + \gamma_{MHD}^2 \left\{ \delta_c + \frac{\delta_{\perp h} + \delta_{\parallel h} - (k_\perp \rho_h)^2 (\beta_h R/2\Delta)}{\left[1 - (2\Delta/R\beta_c)(1 - P'_{\parallel h}/BB') - (k_\perp \rho_h)^2 \beta_h/\beta_c\right]} \right\} = 0 , \qquad (8)$$

where $\gamma_{MHD} = (k/k_\perp)(P'/\rho_m R)^{1/2}$ is the MHD interchange growth rate, $\delta_j = P'_j/P'$ is the pressure gradient fraction, $P = 2P_c + P_{\perp h} + P_{\parallel h}$ is the total pressure, $P' = \partial P/\partial r$, and ω_{*i} is the ion diamagnetic drift frequency. It is assumed that $\Delta_b/R \ll 1$. The hot electron Larmor radius ρ_h is defined by $\rho_h^2 = -M_e(\partial/\partial r)\int d^3v(v_\perp^4/8\omega_{ce}^2)F_h(BB')^{-1}$. From Eq. (8), the interchange mode is unstable in the interval

$$\left(\frac{2\Delta}{R\beta_h}\right)\left(1 + \frac{\delta_{\parallel h}}{\delta_{\perp h}}\right) - \frac{\beta_c}{\beta_h} < k_\perp^2 \rho_h^2 < \left(\frac{2\Delta}{R\beta_h}\right)\left(1 + \frac{\delta_{\parallel h}}{\delta_{\perp h}}\right) \qquad (9)$$

which implies a deterioration of the core beta limit of the interacting ring-plasma interchange mode due to modest Larmor radius. Since satisfying the left-hand condition of Eq. (9) stabilizes the magnetic compressional mode, the condition

$$(k_\perp \rho_h)^2 > \left(\frac{2\Delta}{R\beta_h}\right)\left(1 + \frac{\delta_{\parallel h}}{\delta_{\perp h}}\right) \tag{10}$$

is sufficient for hot electron gyro-radius stabilization of all low frequency modes. In addition, finite ion gyro-radius stabilization of interchange occurs if

$$\frac{1}{4}\left(\frac{\omega_{*i}}{\gamma_{MHD}}\right)^2 > \delta_c + \frac{\delta_{\perp h} + \delta_{\parallel h} - (k_\perp \rho_h)^2(\beta_h R/2\Delta)}{\left[1 - (2\Delta/\beta_c R)\left(1 - P'_{\parallel h}/BB'\right) - (k_\perp \rho_h)^2(\beta_h/\beta_c)\right]}, \tag{11}$$

which can be quite effective for finite $k_\perp$ (except near the transition where the compressional mode is just stabilized). The line-averaged generalizations of Eqs. (8)-(11) yield similar stability criteria, being heavily weighted by the hot electron pressure.

The low frequency hot electron finite Larmor stabilization[6] is illustrated in Fig. 2. These plots were obtained from a local dispersion relation derived for $E_\parallel = 0$, cold ions ($T_i = 0$), high parallel phase velocity, long-thin approximation ($B'/B \gg R^{-1}$), isotropic plasma electrons with density n_e and temperature T_e, and bi-Maxwellian ring electrons (n_i, $T_{\perp h}$, $T_{\parallel h}$). Typical EBT-S parameters ($\Delta/R = 0.05$, $n_h/n_i = 0.1$, $\Delta = 2$ cm, $\rho_h = 0.3$ cm, $k_\perp = m/a$) were used. Figure 3 shows that anisotropy lowers the core beta limit below $\beta_c = 4\Delta/R$, but enhances compressional mode stability. Also, a new stable region due to finite Larmor radius appears for m = 20, after stability had deteriorated for intermediate m values--in accordance with the predictions of Eqs. (9) and (10).

Examination of the high frequency modes ($\omega/\omega_{ci} \gg 1$) shows that the hot electron interchange is stable if

$$\mathrm{FR} \equiv \frac{(k_\perp \rho_h)^2 R\beta_h}{2\Delta(1 + \delta_{\parallel h}/\delta_{\perp h})} > 1 - \frac{(k_\perp/k)^2}{4q_0(1 - \tilde{\beta}_c)} , \qquad (13)$$

whereas the compressional Alfvén mode is stable if $\mathrm{FR} > 1$, as before in Eq. (10). Furthermore, with hot electron finite Larmor radius, the high-frequency coalescence of modes stated earlier and concomitant loss of stability can be avoided if $\mathrm{FR} > 1 - (k_\perp/k)^2[q_0(1 - \beta_c)]^{-1}$. Thus, the condition in Eq. (10) is sufficient to stabilize <u>all</u> curvature-driven modes in EBT, high frequency compared to ω_{ci} as well as low frequency.

V. CONCLUSIONS

A new energy principle for low frequency fluctuations predicts that EBT is unstable provided the constraint $\partial F/\partial E|_J < 0$. Experimentally it appears that such modes are not having a strong effect on present-day EBT operation. However, one can correlate the theory with experiment by observing that there is a wide band of parameter space where instability is of a residual wave-particle nature. One may then expect a low level of fluctuation for such modes. Alternatively, the nature of creating an EBT ring is such that it is not clear that $\partial F/\partial E|_J < 0$ is truly satisfied in experiment. In particular, lower energy-ring particles may not be monotonically decreasing functions of energy, and perhaps absolute stability windows for these modes can yet be found.

In the zero Larmor radius radial stability analysis, we observed that although there was a wide parameter range of stability, there exists a parameter band where stability completely deteriorates. The electron finite Larmor radius theory shows that a stability window can re-emerge. There has been experimental evidence of the high frequency hot electron interchange mode. Using nominal EBT-S parameters ($\Delta = 1$ cm, $R = 20$ cm, $T_h = 500$ keV, $\beta_h \simeq 0.5$, $a = 10$ cm) we find that the FLR parameter, FR [Eq. (13)] needs to be larger than 0.4 to open a stability window and greater than 0.65 to stabilize the hot electron interchange mode completely. If we assume $k_r\Delta = 2$ (derived from a single analytic model) we find that the FLR parameter is 1.7 , sufficient to completely stablize the WKB modes. However, as experimental evidence for the hot electron interchange is present, this indicates that either some of the assumed parameters chosen are somewhat different, or a more accurate analysis of the modal structure will show that smaller k_r can be established.

In general, one expects two different stability pictures, depending on whether $\mathrm{FR} \gtrsim 1$ or $\mathrm{FR} \ll 1$. In the former case, all WKB-like modes can be stabilized by FLR theory. Only the longer wavelength layer mode is succeptible to instability.

Presumably, the FLR effects on this mode will be negligible, although the detailed stability analysis is yet to be performed. Hence, the stability limit should be that in Eq. (7), which is no larger than the Nelson-Lee-Van Dam limit. EBT-S experiments tend to be in the regime FR $\gtrsim 1$, but experiments with increasing scale, such as EBT-P and reactor size experiments, will have FR $\ll 1$. Possibly, with hot ion rings, one can design parameters in the large FR regime, where all modes but the rigid layer modes are FLR stabilized. If we assume that the core beta of Eq. (2) limit applies to the layer mode, we see that one cannot use very thin rings to achieve stable containment for a large β_c .

When FR $\ll 1$, there are always modes that will tap the interacting ring-plasma interchange mode. The wavenumbers exist in a band given by Eq. (9). At very low β_c , the wavenumber width of the unstable band, $\delta k_\perp$, can be quite small, $\delta k_\perp / k_\perp \simeq \beta_c / 2\beta_h$, but as β_c increases, the band width of instability will become substantial. As $k_\perp$ can be quite large, this mode will probably give rise to enhanced diffusion. Further study is needed to quantify diffusion rates.

REFERENCES

[1] ANTONSEN, T. M. and LEE, Y. C., Phys. Fluids 25, 132 (1982).
[2] VAN DAM, J. W., et al., to appear in Phys. Fluids (August 1982).
[3] ANTONSEN, T. M. and LEE, Y. C., in Proc. 2d Hot Electron Ring Physics Workshop (ORNL, 1982), ed. N. A. Uckan, CONF-811203.
[4] BERK, H. L., et al., to be published in Phys. Fluids.
[5] NGUYEN, K. T., et al., in Proc. 2d Hot Electron Ring Physics Workshop, (ORNL, 1982), ed. N. A. Uckan, CONF-811203.
[6] TSANG, K. T. and CATTO, P. J., Science Applications, Inc., Report PRI-34 (1981).
[7] BALDWIN, D. E., and BERK, H. L., private communication.
[8] UCKAN, N. A., to be published in Plasma Physics.

Research sponsored by:
Institute for Fusion Studies: U. S. Dept. of Energy, contract DE-FG05-80ET-53088 with UT Austin and by University of Texas Program Development Fund.
Oak Ridge National Laboratory: Office of Fusion Energy (ETM), U. S. Dept. of Energy, contract W-7405-eng-26 with Union Carbide Corporation.
University of Maryland Dept. of Physics and Astronomy: U. S. Dept. of Energy and the National Science Foundation.
Science Applications, Inc.: U. S. Dept. of Energy contract DE-AC03-76-ET-53057.
University of Michigan, Dept. of Nuclear Engineering: U. S. Dept. of Energy.

FIGURE CAPTIONS

Fig. 1 Marginal stability curves neglecting FLR effects for short wavelength WKB modes, calculated using EBT-P parameters for indicated mode numbers.

Fig. 2 Boundaries of stable operating window in n_c/n_h vs. q_0 space for a reactor near interacting pressure mode. Lower limit on β_h determined from background pressure interchange mode and upper limit on β_h determiined by ring-power requirements.

Fig. 3 Plot of marginal stability boundaries for low frequency finite Larmor radius stability for m = 5 (dotted), m = 10 (solid), and m = 20 (dashed) lines.

Table I. STABILITY CONDITIONS FOR WKB MODES

Mode	Stability Condition	Maximum Growth Rate $\mathrm{Im}(\omega/\omega_{ci})$	Marginal Frequency $\mathrm{Re}(\omega/\omega_{ci})$
MHD Hot Electron Interchange ($\omega/\omega_{ci} < 1$)	$\frac{n_h}{n_i} < \frac{(k_\perp \Delta)^2}{4} q_0 (1-\tilde{\beta}_c)^2$	$\left(\frac{n_h}{n_i} q_0\right)^{1/2} \frac{k}{k_\perp}$	$\left(\frac{k\Delta}{2}\right) q_0$
High-Frequency Hot Electron Interchange ($\omega/\omega_{ci} \gtrsim 1$)	$q_0 < 1/4$ or $\frac{n_h}{n_i} < \left(1 - \frac{k_\perp}{q_0^{1/2} k}\right)^2$	$q_0^{1/2} k_\perp \Delta$	$q_0^{1/2} k_\perp \Delta$
Compressional Wave	$\frac{n_h}{n_i} > \frac{k^2 q_0 \beta_h^2 (1-\tilde{\beta}_h^{-1})(1-\tilde{\beta}_c)}{k_\perp^2 [(q_0 k^2/k_\perp^2)(1-\tilde{\beta}_c)-1]^2}$	$\frac{2k_\perp \Delta (q_0 n_h/n_i)^{1/2}}{\beta_h (1-\tilde{\beta}_h^{-1})}$	$\frac{2k\Delta q_0}{(1+q_0 k^2/k_\perp^2)}$
Background Pressure Interchange Mode ($\omega/\omega_{ci} << 1$)	$\beta_h > 4\Delta/R$ or $\frac{n_h}{n_i} > 2\sqrt{2} k_\perp \Delta \left(\frac{q_0 T_c}{T_h}\right)^{1/2} \left(1 - \frac{\tilde{\beta}_h}{2}\right)^{1/2}$	$\frac{\sqrt{2}k}{k_\perp}\left(\frac{q_0 T_c}{T_h}\right)^{1/2}\left(1-\frac{\tilde{\beta}_h}{2}\right)^{1/2}$	$\frac{\sqrt{2}k}{k_\perp}\left(\frac{q_0 T_c}{T_h}\right)^{1/2}\left(1-\frac{\tilde{\beta}_h}{2}\right)^{1/2}$
Interacting Pressure Mode ($\omega/\omega_{ci} < 1$)	$\beta_c < \frac{2\Delta}{R} (1+P_{\parallel h}/P_{\perp h})$	$\sqrt{\frac{3}{2}} k\Delta \left(\frac{q_0}{k_\perp \Delta}\right)^{2/3} \left[\frac{n_h}{n_i}\left(1-\frac{2}{\tilde{\beta}_h}\right)\right]^{1/3}$	$\sqrt{2} k\Delta \left(\frac{q_0}{k_\perp \Delta}\right)^{2/3} \left[\frac{n_h}{n_i}\left(1-\frac{2}{\tilde{\beta}_h}\right)\right]^{1/3}$

where $\tilde{\beta}_h = \beta_h (R/2\Delta)$, $\tilde{\beta}_c = \beta_c (R/2\Delta)$

EBT-P STABILITY REGIONS
(T_{CORE} = 10 keV)

ORNL-DWG 81-17074R FED

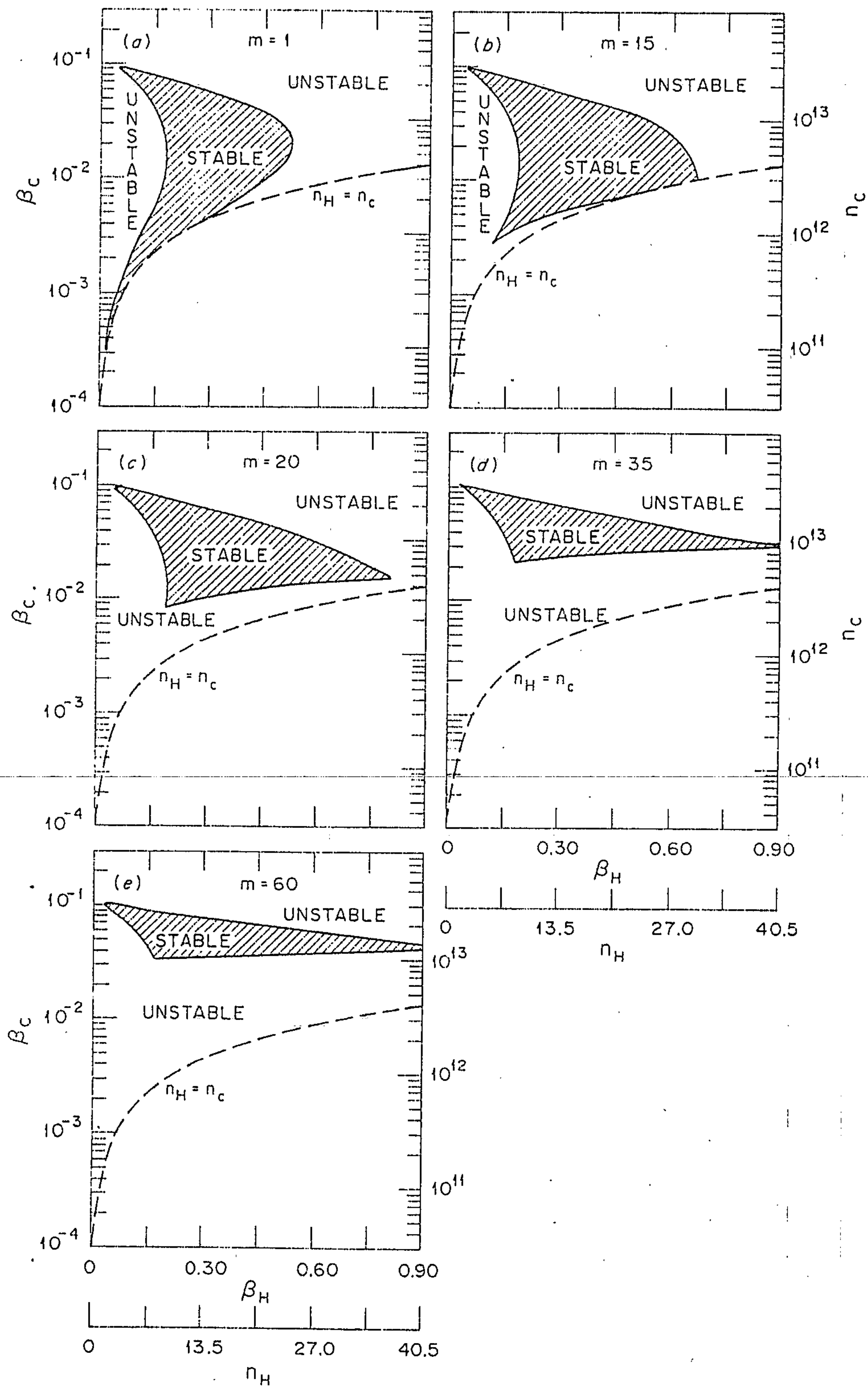

Fig. 1

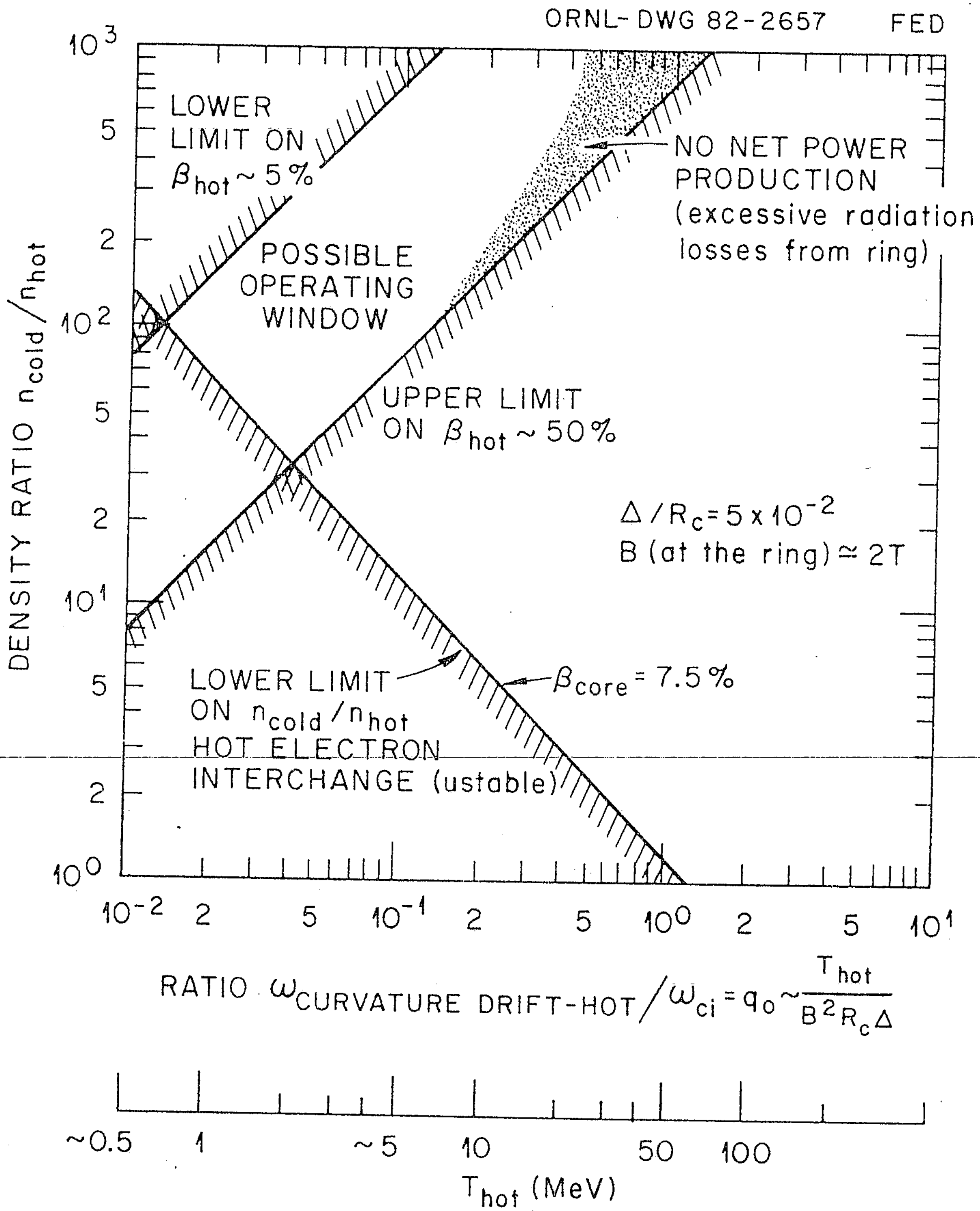
ORNL-DWG 82-2657 FED
LOWER LIMIT ON $\beta_{hot} \sim 5\%$
POSSIBLE OPERATING WINDOW
NO NET POWER PRODUCTION (excessive radiation losses from ring)
UPPER LIMIT ON $\beta_{hot} \sim 50\%$
$\Delta / R_c = 5 \times 10^{-2}$
B (at the ring) $\simeq$ 2T
LOWER LIMIT ON n_{cold}/n_{hot} HOT ELECTRON INTERCHANGE (ustable)
$\beta_{core} = 7.5\%$
DENSITY RATIO n_{cold}/n_{hot}
RATIO $\omega_{CURVATURE\ DRIFT-HOT}/\omega_{ci} = q_0 \sim \frac{T_{hot}}{B^2 R_c \Delta}$
T_{hot} (MeV)
~0.5
1
~5
10
50
100

Fig. 2

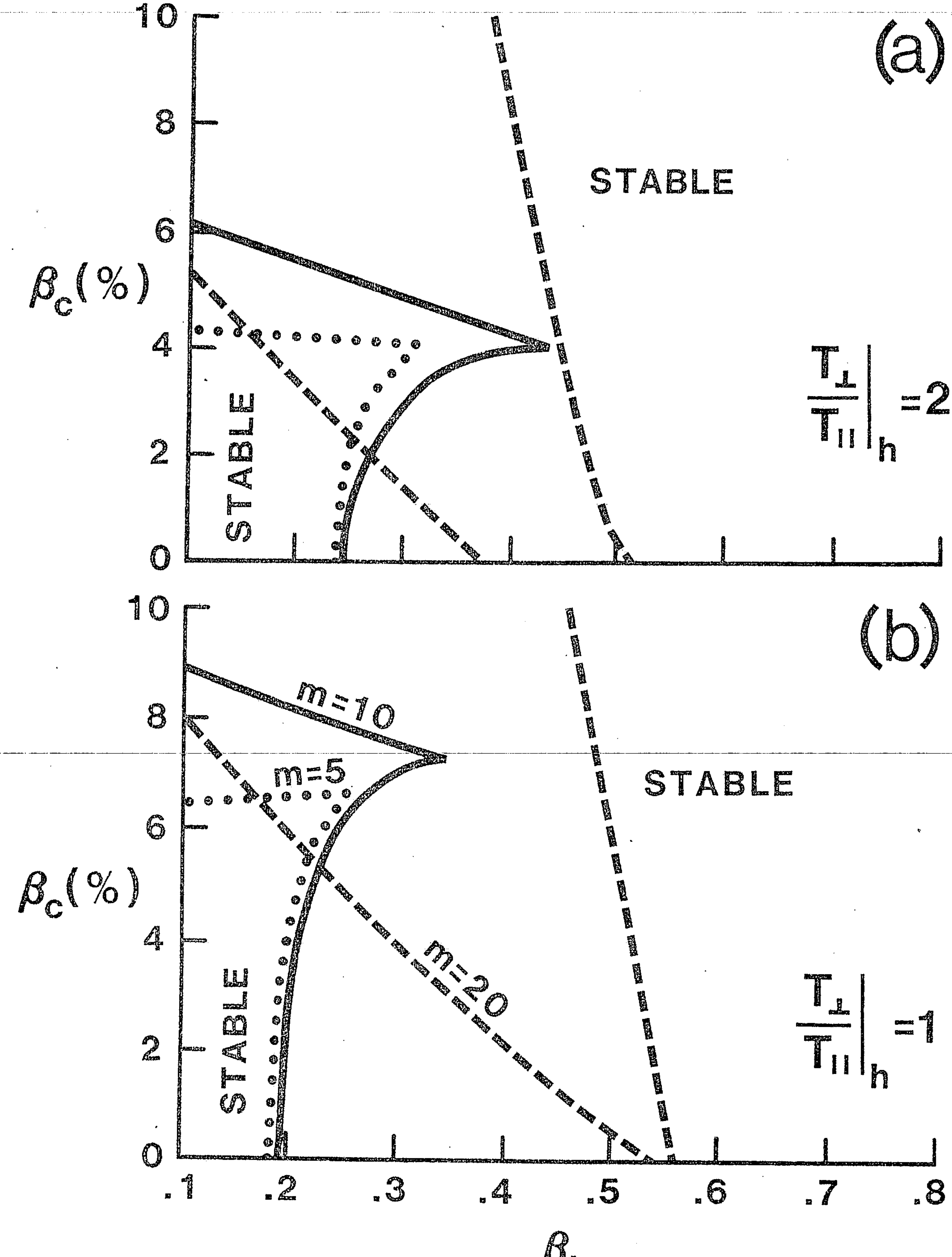

(a)
STABLE
STABLE
$\frac{T_\perp}{T_\parallel}\Big|_h = 2$
$\beta_c(\%)$
10
8
6
4
2
0
(b)
m=10
m=5
m=20
STABLE
STABLE
$\frac{T_\perp}{T_\parallel}\Big|_h = 1$
$\beta_c(\%)$
10
8
6
4
2
0
.1
.2
.3
.4
.5
.6
.7
.8
β_h

Fig. 3

Table I. STABILITY CONDITIONS FOR WKB MODES

Mode	Stability Condition	Maximum Growth Rate $\mathrm{Im}(\omega/\omega_{ci})$	Marginal Frequency $\mathrm{Re}(\omega/\omega_{ci})$
MHD Hot Electron Interchange ($\omega/\omega_{ci} < 1$)	$\frac{n_h}{n_i} < \frac{(k_\perp \Delta)^2}{4} q_0 (1-\tilde{\beta}_c)^2$	$\left(\frac{n_h}{n_i} q_0\right)^{1/2} \frac{k}{k_\perp}$	$\left(\frac{k\Delta}{2}\right) q_0$
High-Frequency Hot Electron Interchange ($\omega/\omega_{ci} \gtrsim 1$)	$q_0 < 1/4$ or $\frac{n_h}{n_i} < \left(1 - \frac{k_\perp}{q_0^{1/2} k}\right)^2$	$q_0^{1/2} k_\perp \Delta$	$q_0^{1/2} k_\perp \Delta$
Compressional Wave	$\frac{n_h}{n_i} > \frac{k^2 q_0 \beta_h^2 (1-\tilde{\beta}_h^{-1})(1-\tilde{\beta}_c)}{k_\perp^2 [(q_0 k^2/k_\perp^2)(1-\tilde{\beta}_c)-1]^2}$	$\frac{2k_\perp \Delta (q_0 n_h/n_i)^{1/2}}{\beta_h (1-\tilde{\beta}_h^{-1})}$	$\frac{2k\Delta q_0}{(1+q_0 k^2/k_\perp^2)}$
Background Pressure Interchange Mode ($\omega/\omega_{ci} << 1$)	$\beta_h > 4\Delta/R$ or $\frac{n_h}{n_i} > 2\sqrt{2} k_\perp \Delta \left(\frac{q_0 T_c}{T_h}\right)^{1/2} \left(1 - \frac{\tilde{\beta}_h}{2}\right)^{1/2}$	$\frac{\sqrt{2}k}{k_\perp} \left(\frac{q_0 T_c}{T_h}\right)^{1/2} \left(1 - \frac{\tilde{\beta}_h}{2}\right)^{1/2}$	$\frac{\sqrt{2}k}{k_\perp} \left(\frac{q_0 T_c}{T_h}\right)^{1/2} \left(1 - \frac{\tilde{\beta}_h}{2}\right)^{1/2}$
Interacting Pressure Mode ($\omega/\omega_{ci} < 1$)	$\beta_c < \frac{2\Delta}{R} (1+P_{\parallel h}/P_{\perp h})$	$\sqrt{\frac{3}{2}} k\Delta \left(\frac{q_0}{k_\perp \Delta}\right)^{2/3} \left[\frac{n_h}{n_i}\left(1 - \frac{2}{\tilde{\beta}_h}\right)\right]^{1/3}$	$\sqrt{2} k\Delta \left(\frac{q_0}{k_\perp \Delta}\right)^{2/3} \left[\frac{n_h}{n_i}\left(1 - \frac{2}{\tilde{\beta}_h}\right)\right]^{1/3}$

where $\tilde{\beta}_h = \beta_h (R/2\Delta)$, $\tilde{\beta}_c = \beta_c (R/2\Delta)$